these clusters. For $n \gtrsim 20$ the mass distribution strongly depends on the formation conditions and is mainly determined by the growth statistics. This is confirmed by the fact that the high-mass end of the distribution shifts to smaller masses with decreasing evaporation temperature but leaving the relative intensities for $n \lesssim 20$ nearly unchanged.

In summary, the essential preconditions necessary for systematic investigations of physical properties of particles in the size range between single atoms and the solid state is fulfilled, namely the production of metal clusters, their individual detection and the separation of beams with uniform cluster size. Thus, besides a further detailed investigation of the production process, the development of the collective phenomena, characteristic for the solid, can be studied as a function of particle size.

We acknowledge the help of O. Echt, P. Pfau, and A. Reyes Flotte. This work was partly supported by the Deutsche Forschungsgemeinschaft.

[1]C. G. Granqvist and R. A. Buhrmann, J. Appl. Phys. 47, 2200 (1976).

[2]H. Fröhlich, Physica (Utrecht) 4, 406 (1937); R. Kubo, J. Phys. Soc. Jpn. 17, 975 (1962); L. P. Gor'kov and G. M. Eliasberg, Zh. Eksp. Teor. Fiz. 48, 1407 (1965) [Sov. Phys. JETP 21, 940 (1965)].

[3]F. Meier and P. Wyder, Phys. Rev. Lett. 30, 181 (1973); P. Yee and W. D. Knight, Phys. Rev. B 11, 3261 (1975); C. G. Granqvist, R. A. Buhrmann, J. Wyns, and A. J. Siervers, Phys. Rev. Lett. 37, 625 (1976).

[4]K. Kimoto and I. Nishida, J. Phys. Soc. Jpn. 42, 2071 (1977).

[5]A. Herrmann, S. Leutwyler, E. Schumacher, and L. Wöste, Helv. Chim. Acta 61, 453 (1978).

[6]W. D. Knight, R. Monot, E. R. Dietz, and A. R. George, Phys. Rev. Lett. 40, 1324 (1978).

[7]M. Leleuter and P. Joyes, Radiat. Eff. 18, 105 (1973).

[8]W. Romanowski, Surf. Sci. 18, 373 (1969); M. R. Hoare and P. Pal, Adv. Phys. 24, 645 (1975).

[9]J. Smith and J. G. Gay, Phys. Rev. B 12, 4238 (1975); R. P. Messner, S. K. Knudson, K. H. Johnson, J. B. Diamond, and C. Y. Yang, Phys. Rev. B 13, 1396 (1976); R. O. Jones, P. J. Jennings, and G. S. Painter, Surf. Sci. 53, 409 (1975).

[10]M. Torrini and E. Zanazzi, J. Phys. C 9, 63 (1976).

[11]K. Sattler, J. Mühlbach, A. Reyes Flotte, and E. Recknagel, to be published.

[12]Flow characteristics in the condensation region have been observed by light scattering on small particles: S. Kasukabe, S. Yatsuga, and R. Uyeda, Jpn. J. Appl. Phys. 13, 1714 (1974).

[13]R. Becker and W. Döring, Ann. Phys. (Leipzig) 24, 719 (1935); F. Kuhrt, Z. Phys. 131, 185 (1952); J. Feder, K. C. Russel, L. Lothe, and P. M. Pound, Adv. Phys. 15, 111 (1966); D. Kashchiev, Surf. Sci. 18, 389 (1969); K. Binder and D. Stauffer, Adv. Phys. 25, 343 (1976).

Adatom Configurations of H(2×6) and H(2×1) on Ni(110) Analyzed Using He Diffraction

K. H. Rieder and T. Engel
IBM Zurich Research Laboratory, CH-8803 Rüschlikon, Switzerland

(Received 25 January 1980)

The first determination of *two-dimensional* adsorbate-induced corrugation functions from He-diffraction data is reported. Local maxima in the corrugations of both H(2×6) and H(2×1) on Ni(110) directly reflect adatom positions due to the localized charge distribution of the chemisorbed H atoms. Hence, genuine information on the adsorption sites is obtained leading to novel insight into coverage and adsorbate-adsorbate interactions. The transition to the reconstructed (1×2) saturation phase is discussed.

PACS numbers: 68.20.+t, 82.65.Nz

Although H adsorption on metal surfaces is of high current interest both theoretically (e.g., chemisorption-model system)[1,2] and for technical reasons (surface chemistry, H uptake in metals),[3] only one low-energy electron-diffraction (LEED) study concerning the surface location of H has been published.[4] LEED is of limited use here as H atoms scatter electrons very weakly, and additional diffraction features are extremely faint unless the H adsorption is accompanied by a reconstruction of the substrate.[5,6] On the other hand, the corrugation function obtained from He diffraction is a replica of the surface charge density,[7] and undergoes severe changes upon adsorption of any substance.[8] In our previous He-diffraction study of H(1×2) on Ni(110),[9] the surface structure remained unsolved, as several models were consistent with the one-dimensional corrugation ob-

served. In this paper, we emphasize a crucial aspect for He diffraction as an effective tool of surface crystallography: The electronic charge induced by the chemisorption bond is localized around the adsorbate position, as long as the adsorbate atoms are sufficiently far apart[1,2,8]; the corrugation is then two-dimensional and its local maxima can be associated with underlying adsorbate atoms.[7,8] Thus, the corrugation function yields a direct picture of the adsorption sites, and the coverage can be obtained simply by counting adatoms per unit cell.

We illustrate this important aspect by presenting the two-dimensional adsorbate-induced corrugations for the 2×6 and 2×1 phases of H on Ni(110) deduced from He-diffraction data. These phases appear at smaller coverages than the above-mentioned 1×2 phase, which corresponds to H saturation and involves substrate reconstruction.[5,6] Detection of the H(2×6) phase, which was not observed with LEED,[5] proves the sensitivity of He scattering to delicate adsorption structures as well as its nondestructive nature. Moreover, the successful analysis of the 2×6 structure containing as many as ten adatoms per unit cell demonstrates that He diffraction can be used to tackle complex unit cells (at least for systems with small corrugations).[10]

Figure 1(a) shows in-plane and out-of-plane scattering from the 2×1 structure formed after exposure to 0.7 L H_2 at 100 K for the beam incident along the [001] azimuth. [1 L (langmuir) = 1 μTorr sec.] For experimental details, see Ref. 9. The systematic absence of the $(\pm\frac{1}{2},0)$ beams

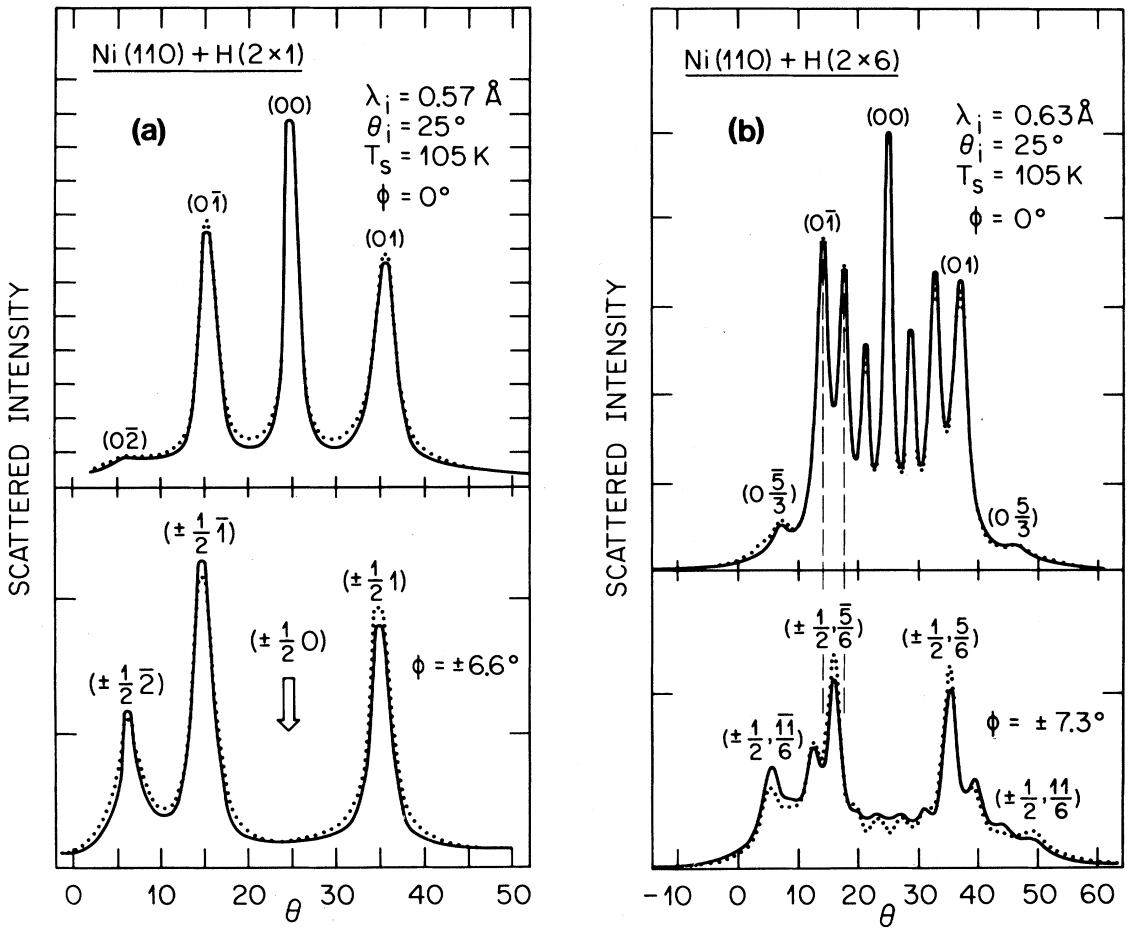

FIG. 1. Scattered He intensity as a function of the scattering angle θ for in-plane and out-of-plane ($\varphi \neq 0$) detection for the (a) 2×1 and (b) 2×6 structures. φ denotes the angle through which the detector is rotated out of plane. The vertical scale unit corresponds to the same intensity for all curves. The (00) beam for the experimental (solid line) and calculated intensity curves (dot line) have been set equal. The total elastically scattered intensity is approximately 30% of the incoming intensity.

indicates that the unit cell is nonprimitive and contains glide lines parallel to the close-packed nickel rows. Also shown in Fig. 1(a) are calculated intensity curves obtained within the eikonal approximation.[10] The effect of the attractive well (~ 10 meV deep)[11] can be neglected relative to the energy of the incoming He atoms (~ 60 meV). Furthermore, because of the low sample temperature and the small $\vec{G}$ vectors involved in the diffraction, the angular-dependent Debye-Waller correction has been neglected. The corrugation function compatible with the glide-line symmetry can be written as

$$\zeta(x,y) = -\tfrac{1}{2}\sum_{l}\zeta(0,l)\cos 2\pi\frac{ly}{a_2} + \sum_{m,n}\zeta(m,n)\sin 2\pi\frac{mx}{a_1}\sin 2\pi\frac{ny}{a_2}. \quad (1)$$

Here, $\vec{a}_1$ and $\vec{a}_2$ denote the unit-cell vectors of the clean Ni(110) surface in $x = [1\bar{1}0]$ and $y = [001]$ directions, respectively, and $\zeta(n,m)$ the Fourier coefficient corresponding to $G = n\vec{a}_1 + m\vec{a}_2$. The best-fit parameters obtained by fitting diffraction spectra at seven angles of incidence between 25° and 50° (relative to the surface normal) with the beam incident along both [001] and $[1\bar{1}0]$ directions are: $\zeta(0,1) = 0.10 \pm 0.02$ Å, $\zeta(0,2) = 0.03 \pm 0.01$ Å, $\zeta(\frac{1}{2},1) = 0.07 \pm 0.01$ Å, and $\zeta(\frac{1}{2},2) = 0.02 \pm 0.01$ Å. These are all coefficients significantly different from zero.

The corrugation surface is shown in Fig. 2(a). The maximum amplitude is 0.26 ± 0.02 Å as compared with 0.05 ± 0.01 Å for the clean surface. As emphasized in the introduction, the maxima can be attributed to the localization of charge induced by the chemisorption bond and to the position of the underlying hydrogen atom. The geometric arrangement of the maxima is shown by the filled circles in the structural model of Fig. 2(b). The registry of the adlayer to the substrate is fixed in the [001] direction by the phase of the $\zeta(\frac{1}{2},1)$ term relative to $\zeta(0,1)$, the only nonzero coefficient[9] for the clean substrate. The registry along $[1\bar{1}0]$ cannot be uniquely determined because of the weak substrate corrugation, and we have chosen the configuration yielding equivalent sites of highest possible coordination. With this choice, the hydrogen atoms are alternately located at distances $(0.25 \pm 0.03)a_2$ from the nickel rows at sites with nearly threefold coordination. This configuration corresponds to a distorted hexagonal close packing of the H atoms with a coverage of one monolayer, and maximizes the distance between H atoms which on Ni(111) have

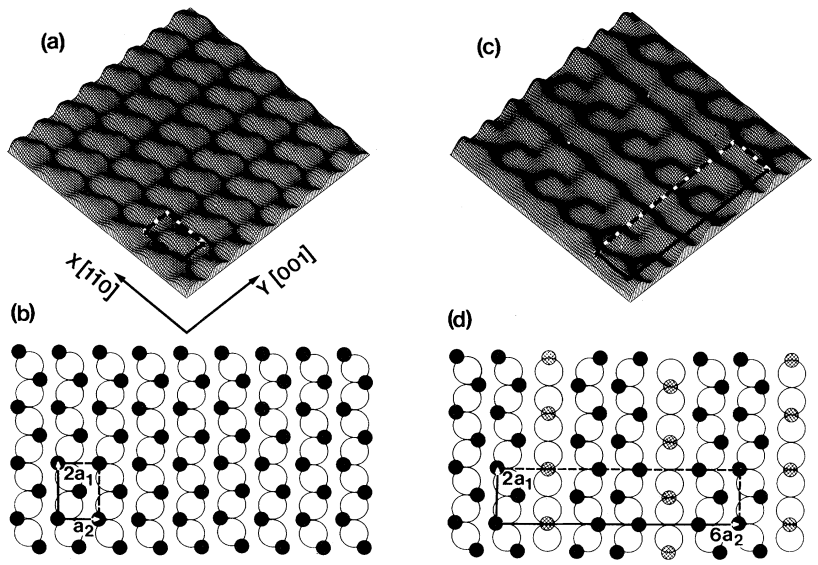

FIG. 2. Best-fit corrugation surfaces for the (a) 2×1 and (c) 2×6 structures. Corresponding hard-spheres models show the adsorption sites for the (b) 2×1 and (d) 2×6 structures. The small filled and shaded circles represent H atoms and the large circles the outermost layer of the Ni(110) substrate. $\vec{a}_1$ and $\vec{a}_2$ are the unit-cell vectors for the Ni(110) surface in the $[1\bar{1}0]$ and [001] directions, respectively. The unit cells of the ordered phases are shown in all figures.

a predominantly repulsive interaction.[4]

Figure 1(b) shows in-plane and out-of-plane diffraction obtained from the 2×6 structure formed after exposure to 0.5 L H_2 at 100 K. The hydrogen coverage as determined by thermal desorption is 80% that of the 2×1 structure. Particularly striking is the pronounced rainbow scattering in plane, and the absence of odd sixth-order peaks in plane and of even sixth-order peaks out of plane. Also shown in Fig. 1(b) are intensity curves calculated using Eq. (1) as outlined above. The best-fit parameters obtained for three different angles of incidence between 25° and 50° for $\lambda = 0.57$ Å and for the data shown in Fig. 1(b) are: $\zeta(0,\frac{1}{3}) = -0.09\pm0.02$ Å, $\zeta(0,\frac{2}{3}) = 0.12\pm0.02$ Å, $\zeta(0,1) = 0.09\pm0.02$ Å, $\zeta(\frac{1}{2},\frac{5}{6}) = 0.06\pm0.01$, and $\zeta(\frac{1}{2},\frac{3}{6}) = -0.03\pm0.01$ Å. The corrugation surface is shown in Fig. 2(c). It consists of paired zigzag chains as in Fig. 2(a) with the important difference that alternate chain pairs are phase shifted by the lattice vector $\vec{a}_1$. Additional smaller peaks with a spacing of $2a_1$ along the $[1\bar{1}0]$ direction are seen midway between the chain pairs. The geometrical arrangement of the maxima is indicated by the small filled and shaded circles in Fig. 2(d), and the registry with the substrate has been chosen as for the 2×1 structure. The structure observed is again a distorted hexagonal packing in which two different sites are occupied. This model corresponds to a coverage of 0.83 in good agreement with the experimental determination. The maximum height difference is 0.25 ± 0.02 Å for the atoms in the zigzag chains, and 0.18 ± 0.02 Å for the additional peaks.

This analysis of the 2×6 and 2×1 structures together with that of the 1×2 structure[9] allows a complete description of all homogeneous hydrogen phases formed on Ni(110). Of particular interest is the change in the adatom configuration between different phases as the coverage is increased. The zigzag arrangement with the H atoms in threefold-coordinated sites on the close-packed nickel rows is a highly stable configuration. The lateral interaction of the H atoms is primarily repulsive at small separations, so that nearest-neighbor distances are maximized. This dictates an in-phase arrangement of adjacent zigzag chains for the 2×1 structure in which all such sites are occupied. At lower coverages, not all rows will be filled and the results for the 2×6 structure show that the twofold sites are preferred in unfilled rows despite their smaller binding energy[1]; their smaller corrugation amplitude is in accord with the shorter chemisorption-bond length expected for a twofold site.[1] At a coverage of 0.83, the repulsive interaction between the H atoms at the twofold sites and their neighbors causes the phase shift of $\vec{a}_1$ between adjacent zigzag chain pairs. The adatom configuration in both the 2×6 and 2×1 structures can therefore be understood in terms of the stability of the zigzag arrangement and the repulsive lateral interaction between H atoms.

Since the 2×1 structure corresponds to a completion of the zigzag chains, additional hydrogen can only be adsorbed if the local adsorbate configuration is changed and this change is coupled with a substrate reconstruction in the 1×2 structure.[6] With use of our calibration for the 2×1 structure, the coverage of the 1×2 structure is 1.6 ± 0.1, which is consistent with the high coverage model in Fig. 3(c) of Ref. 9. The adatom position for the 1×2 structure cannot be established as reliably as for the other ordered phases, as only very weak corrugation was detected in the $[1\bar{1}0]$ direction. This shows that an extensive charge redistribution has taken place. However, the maximum height of the corrugation surface for all three ordered phases is 0.25 ± 0.02 Å, substantiating our previous conclusion[9] that the 1×2 corrugation amplitude is primarily due to the adsorbed H atoms rather than to a substrate reconstruction.

In conclusion, we have shown that He diffraction from adsorbate-covered surfaces can give a direct picture of adatom positions through the maxima of the corrugation function. As the form of the corrugation surface reflects the spatial distribution of the surface charge density, it is possible, in principle, to extract details such as bond lengths and charge distribution in the chemisorption bond. However, such an analysis requires better theoretical understanding of the He–solid-surface interaction. In particular, the dependence of the corrugation amplitude on the form of the interaction potential[12] and on the energy of the incoming He,[7] as well as inelastic effects,[13] must be better understood. Nevertheless, the present results show that He diffraction can give unique structural information and is especially valuable for the investigation of H-adsorption systems.

We thank W. Stocker for technical assistance, H. Thomas for help with the plot program, and A. Baratoff and E. Courtens for valuable discussions.

[1]T. H. Upton and W. A. Goddard, III, Phys. Rev. Lett. 42, 472 (1979).

[2]S. G. Louie, Phys. Rev. Lett. 42, 476 (1979).

[3]P. J. Feibelman, Bull. Am. Phys. Soc. 25, 403 (1980); L. C. Feldman, Bull. Am. Phys. Soc. 25, 403 (1980); J. W. Davenport, Bull. Am. Phys. Soc. 25, 403 (1980); B. R. Livesay, Bull. Am. Phys. Soc. 25, 404 (1980); G. K. Shenoy, Bull. Am. Phys. Soc. 25, 404 (1980).

[4]K. Christmann, R. J. Behm, G. Ertl, M. A. Van Hove, and W. H. Weinberg, J. Chem. Phys. 70, 4168 (1979).

[5]N. Taylor and P. J. Estrup, J. Vac. Sci. Technol. 11, 244 (1974).

[6]J. Demuth, J. Colloid. Interface Sci. 58, 184 (1977).

[7]N. Esbjerg and J. K. Nørskov, Phys. Rev. Lett. 45, 807 (1980) (this issue).

[8]N. O. Lang and A. R. Williams, Phys. Rev. Lett. 37, 212 (1976).

[9]K. H. Rieder and T. Engel, Phys. Rev. Lett. 43, 373 (1979).

[10]U. Garibaldi, A. C. Levi, R. Spadacini, and G. E. Tommei, Surf. Sci. 48, 649 (1975).

[11]J. M. Soler, N. Garcia, V. Celli, K. H. Rieder, and T. Engel, in Proceedings of the Third European Conference on Surface Science/Fourth International Conference on Solid Surfaces, Cannes, France, 1980 (to be published).

[12]G. Armand and J. R. Manson, Phys. Rev. Lett. 43, 1839 (1979).

[13]A. C. Levi and H. Suhl, Surf. Sci. 88, 221 (1979).

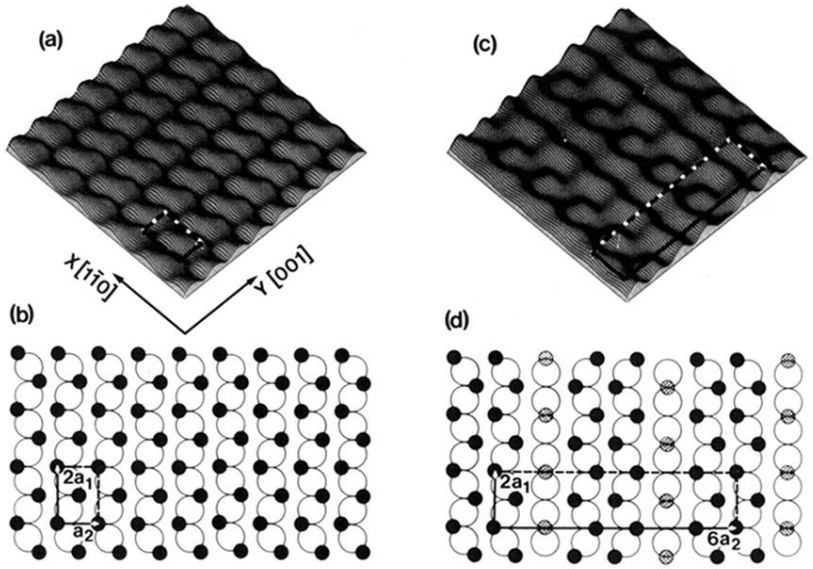

FIG. 2. Best-fit corrugation surfaces for the (a) 2×1 and (c) 2×6 structures. Corresponding hard-spheres models show the adsorption sites for the (b) 2×1 and (d) 2×6 structures. The small filled and shaded circles represent H atoms and the large circles the outermost layer of the Ni(110) substrate. $\vec{a}_1$ and $\vec{a}_2$ are the unit-cell vectors for the Ni(110) surface in the $[1\bar{1}0]$ and [001] directions, respectively. The unit cells of the ordered phases are shown in all figures.